Ecology, 93(5), 2012, pp. 1214–1227

Consistent scaling of persistence time in metapopulations

GUR YAARI,[1,4] YOSSI BEN-ZION,[2] NADAV M. SHNERB,[2] AND DAVID A. VASSEUR[3]

[1]*Department of Pathology Informatics, Yale University School of Medicine, New Haven, Connecticut 06511 USA*
[2]*Department of Physics, Bar-Ilan University, Ramat Gan 52900 Israel*
[3]*Department of Ecology and Evolutionary Biology, Yale University, New Haven, Connecticut 06520 USA*

Abstract. Recent theory and experimental work in metapopulations and metacommunities demonstrates that long-term persistence is maximized when the rate at which individuals disperse among patches within the system is intermediate; if too low, local extinctions are more frequent than recolonizations, increasing the chance of regional-scale extinctions, and if too high, dynamics exhibit region-wide synchrony, and local extinctions occur in near unison across the region. Although common, little is known about how the size and topology of the metapopulation (metacommunity) affect this bell-shaped relationship between dispersal rate and regional persistence time. Using a suite of mathematical models, we examined the effects of dispersal, patch number, and topology on the regional persistence time when local populations are subject to demographic stochasticity. We found that the form of the relationship between regional persistence time and the number of patches is consistent across all models studied; however, the form of the relationship is distinctly different among low, intermediate, and high dispersal rates. Under low and intermediate dispersal rates, regional persistence times increase logarithmically and exponentially (respectively) with increasing numbers of patches, whereas under high dispersal, the form of the relationship depends on local dynamics. Furthermore, we demonstrate that the forms of these relationships, which give rise to the bell-shaped relationship between dispersal rate and persistence time, are a product of recolonization and the region-wide synchronization (or lack thereof) of population dynamics. Identifying such metapopulation attributes that impact extinction risk is of utmost importance for managing and conserving the earth's evermore fragmented populations.

Key words: demographic stochasticity; extinction prone; metapopulation; scaling; synchronization.

INTRODUCTION

The concept of the metapopulation, a set of local patches of a single species that are linked by dispersal (Levins 1969, Hanski and Gilpin 1991, Hanski and Ovaskainen 2000), has been an important contributor to our understanding of how biological populations persist, particularly in harsh environments where localized extinctions are common. More recently, metapopulations have been embedded into metacommunities, where local patches comprise pairs or sets of interacting species (Holyoak and Lawler 1996, Burkey 1997, Kerr et al. 2002, 2006, Holyoak et al. 2005). Classic metapopulation theory used a patch–occupancy approach to determine how the rates of colonization and extinction impacted the fraction of patches in a metapopulation that were occupied at a steady state (Levins 1969, 1970). However, the deterministic nature of patch–occupancy models precludes them from estimating the probability of regional extinction, a desirable quantity for management and conservation objectives (Durrett and Levin 1994, Earn et al. 2000). Stochastic patch–occupancy models (SPOMs) have been developed to project the probability that any or all patches will be occupied in the future as a function of local rates of colonization and extinction, which may in turn depend on a variety of factors such as patch quality and connectivity (Etienne et al. 2004). SPOMs are more tractable than individual-based models, which are hampered by large numbers of parameters; however, they lack the explicit population dynamics which give rise to "mass effects," a net flow of dispersing individuals between patches generated by local differences in population size or density (Shmida and Wilson 1985, Holyoak et al. 2005). Mass effects alter the probability of recolonization of a patch after a local extinction because the population dynamics of neighboring patches are not independent, but tend to be synchronized by the action of dispersal; thus, patches in which populations are locally extinct tend be neighbored by others which may also be locally extinct or on the brink of extinction (Heino et al. 1997). Where local environmental heterogeneity acts to maintain local population dynamics in a state of asynchrony (negative correlation; Abta et al. 2007, 2008), local extinctions are often avoided altogether by the inflow of individuals from nearby patches where populations are at high abundance (Brown and Kodric-Brown 1977).

The importance of synchronization and mass effects in metapopulations and metacommunities has been

---

Manuscript received 14 June 2011; revised 22 September 2011; accepted 22 November 2011. Corresponding Editor: L. Stone.

[4] Email: gur.yaari@yale.edu

most often explored in relation to their effect on the temporal variance of populations at the regional scale (Keeling et al. 2000, Dey and Joshi 2006, Hastings and Wysham 2010, Abbott 2011) and where local temporal variation in population size is maintained by internal instabilities such as cycles or chaos (Allen et al. 1993, Earn et al. 2000). In these circumstances, increasing the synchrony of population dynamics (via increased dispersal among populations or via a global environmental effect) always yields greater variance at the metapopulation level (Loreau et al. 2003).

The link between metapopulation variance and metapopulation persistence is unfortunately less straightforward. In the absence of any movement of individuals among patches (and any widespread environmental factors), asynchronous local dynamics are likely, leading to low metapopulation variance; however, patches in which extinctions have occurred cannot be recolonized and the size of the metapopulation continually shrinks to extinction. Dispersive movement of individuals increases the potential for recolonization, but also synchronizes local dynamics, thereby increasing the temporal variance of the metapopulation and potentially the extinction risk. Researchers often employ the coefficient of variation ($CV = \sigma/\mu$) as a means of estimating extinction risk for populations (e.g., Drake and Griffen 2010) and similar logic has been extended to metapopulations (Holyoak and Lawler 1996). However, the CV may not yield a reliable estimate of extinction risk when nonequilibrium dynamics are important because variation around the deterministic trajectory can vary substantially at different points in time (see section 6 in the Appendix). Studying the trade-off between dispersal and synchronization therefore requires the incorporation of local population dynamics (mass effects) into models where local extinction is a real possibility.

Typically, the types of models used to study mass effects are unsuitable for studying the processes of local and regional extinction because local population dynamics are generated by deterministic models, which themselves do not include extinction as a possible outcome. However, by incorporating stochasticity (and/or a threshold extinction density) into model parameters or population size directly, local and regional persistence has been investigated under the influence of environmental catastrophes (Lande 1993), resource scarcity (Bulte and van Kooten 1999), species interactions (Chesson 2000, Keeling and Gilligan 2000, Keeling 2002), or simply due to random fluctuations in the local rates of birth and death (Lande 1993, Hastings and Wysham 2010). This latter source of local extinctions, termed demographic stochasticity (May 1973) is particularly important when population size is depressed, which can occur as a consequence of predator–prey oscillations (Hinrichsen 2000, Holyoak 2000, Keymer et al. 2000), invasion fronts (Brunet and Derrida 1997, Sokolov et al. 1997, Kessler and Levine 1998), recent establishment (Kessler and Shnerb 2008), or when the landscape is heterogeneous and certain fragments support only a low density (Missel and Dahmen 2008). Given that many, if not all, of these patterns and processes operate locally in metacommunities, demographic stochasticity can have important consequences for dynamics and extinction risk even when the regional population size is large. However, little is known about how dispersal and metapopulation size interactively influence the probability of regional extinction when local dynamics (patches) are prone to extinction due to one or more of the above mechanisms.

Demographic stochasticity has been the subject of intensive research, both empirically (Stacey and Taper 1992, Martin et al. 2000, Bonsall and Hastings 2004, Matthies et al. 2004) and theoretically (Elgart and Kamenev 2004, Kessler and Shnerb 2007, Kamenev and Meerson 2008, Ovaskainen and Meerson 2010). A common approach to modeling demographic stochasticity in deterministic models is to sample the population size, at each time step, from a Poisson distribution with an expected value given by the deterministic model projection from the previous time step (Johst et al. 2002). This generates relatively large variation around the expected population size when it is small and little variation when the expected population size is large, which is consistent with demographic stochasticity. Although this approach works well for discrete-time systems where generations are nonoverlapping, it does not apply to the vast majority of populations, whose generations overlap. Research on the effects of demographic stochasticity on continuous-time models has been particularly lacking, perhaps due to the challenge of discretizing and randomizing the processes of birth and death in continuous time. Lande (1993) approached the issue of modeling demographic stochasticity in a continuous-time model of simple (linear) population growth by sampling the per capita growth rate from a normal distribution with constant mean and a variance inversely related to population size. Under this scenario, stochastic calculus can be used to estimate the mean persistence time. More recently, other methods for estimating mean times to extinction have been shown to be sufficiently accurate for single populations (for review see Ovaskainen and Meerson 2010). However, the accuracy of these methods, and those employed by Lande (1993), is appreciably lower at small population sizes, weakening their utility for metapopulation research. An alternative to directly estimating extinction times is to use a stochastic simulation algorithm (Gillespie 1976) that incorporates the randomness of demographic events in population dynamics and observe the distribution of outcomes. Although computationally expensive, the Gillespie is easily applied to ordinary differential equations, and exactly reproduces their dynamics for large enough population sizes (Legendre et al. 2008, zu Dohna and Pineda-Krch 2010).

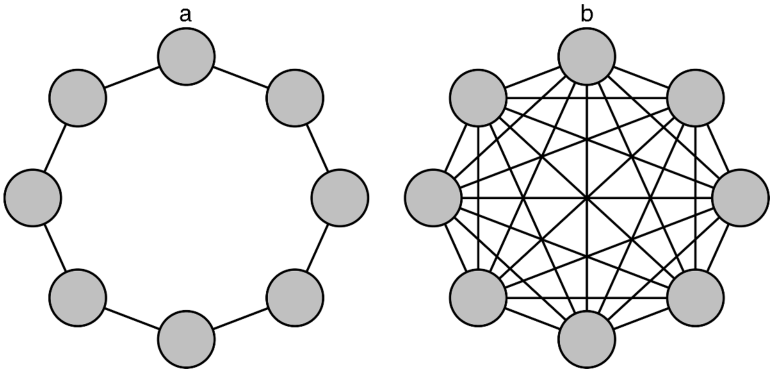

FIG. 1. Examples of how eight patches are interconnected for the (a) stepping-stone (SS) topology and the (b) fully connected (FC) topology.

In this study we investigated the relationship between the mean metapopulation persistence time, dispersal rate, and the number of patches when local population dynamics are subject to demographic stochasticity. Additionally, we examined two metapopulation topologies that form the boundaries for all possible topologies (where dispersal occurs either between all patches or along a stepping-stone pathway; Fig. 1; Earn et al. 2000). To generalize our findings, we modeled local population dynamics using both single-species and two-species (predator–prey and parasite host) models, employing both discrete-time models and two continuous-time approaches. We found that a consistent relationship between metapopulation persistence time and the number of patches emerges in each of three dispersal regimes (low, intermediate, and high), giving rise to the well-known bell-shaped relationship between persistence time and dispersal. Furthermore, we found that metapopulation topology impacts only the parameters of the scaling rate at intermediate dispersal (with no effect on the form of the relationship).

MODELING SCHEMES

Deterministic models

We began with a set of six well-studied deterministic models that provide a mathematical description of the process of population growth in the absence of space and noise. This set of models includes both discrete-time (Logistic map, Ricker map, Nicholson-Bailey host–parasite model) and continuous-time processes (Logistic growth, Lotka-Volterra, and Rosenzweig-MacArthur consumer–resource models; see Table 1) of single-species systems and of two-species enemy–victim systems. This set of deterministic models exhibits a range of different dynamical features that may affect the relationship among the number of metapopulation patches, dispersal rate, system topology, and persistence time of the metapopulation. We discuss these features in the next paragraph.

In general, the six deterministic models can each exhibit a range of qualitative dynamics depending on parameter values. We highlight two general qualitative characteristics under which these models can be categorized: (1) Population density may asymptotically approach the extinction boundary or (2) population density may asymptotically be bounded to a region that does not include extinction boundary. This region may be a stable, nontrivial fixed point (equilibrium), an attractive limit cycle, or a chaos within a bounded range. A crucial point is that these deterministic models themselves never include extinction as a possible outcome; only in the presence of demographic stochasticity is extinction possible. However, it is important to consider that the qualitative behavior of a particular model may make populations more susceptible to extinction (e.g., due to low densities on deterministic population trajectories). Fig. 2 demonstrates the deterministic dynamics of each of these models (on a single site).

To ensure that extinctions are possible, we extended the deterministic framework for each of the six models (Table 1) to include local demographic stochasticity (see Fig. 2 for typical realizations of the stochastic systems). This process requires (1) discretization of the population density in each patch into an integer-measure of population size and (2) a forward projection method which incorporates stochasticity in the processes of birth and death. We implemented demographic stochasticity in different manners for discrete and continuous-time models. We give a brief discussion of these methods in the next subsection and provide a complete description of the process for each model in the Appendix.

Incorporating stochasticity and dispersal

For the discrete-time models, we built upon the simulation techniques presented in Ben-Zion et al. (2010). In general, the number of individuals at time $t + 1 (n_{t+1})$ is a random integer taken from a binomial distribution $B(n_t, p_t)$ where n_t is given by the total number of individuals at time t (including offspring produced by the population at time t), and p_t is the probability that an individual will survive and be counted in the population at time $t + 1$. For example, using the well-known Ricker model,

$$x_{t+1} = x_t \times \exp\left[r\left(1 - \frac{x_t}{\kappa}\right)\right]$$

TABLE 1. Dynamics features of the studied models.

Model (deterministic dynamics)	Equation	Species number	Time update	$X_{\min}$	Parameters
Logistic growth	$\frac{dx}{dt} = \left(\lambda - \mu + \frac{\sigma}{2}\right)x - \frac{\sigma}{2}x^2$	$1(x)$	continuous	$X_{\min} = \frac{\left(\lambda - \mu + \frac{\sigma}{2}\right)}{\frac{\sigma}{2}} = 2$	$\lambda = 0.2,\ \mu = 0.1,$ $\sigma = 0.2$ and 2
Logistic map	$x_{t+1} = rx_t\left(1 - \frac{x_t}{\kappa}\right)$	$1(x)$	discrete	$X_{\min} = 0$ 0 neutral	$r = 4,\ \kappa = 12$
Ricker map	$x_{t+1} = x_t \times \exp\left[r\left(1 - \frac{x_t}{\kappa}\right)\right]$	$1(x)$	discrete	$X_{\min} \approx 0.29$	$r = \log(17) \approx 2.83, \kappa = 4$
Nicholson-Bailey	$H_{t+1} = cH_t e^{-\gamma Pt}$ $P_{t+1} = bH_t(1 - e^{-\gamma P_t})$	$2(H,\ P)$	discrete	$X_{\min} = (0, 0)$ (0, 0) attractive	$b = 1,\ c = 2,\ \gamma = 0.01$
Rosenzweig-MacArthur I	$\frac{dN}{dt} = \left(\lambda - \mu_N + \frac{\sigma}{2}\right)N - \frac{\sigma}{2}N^2 - \frac{\gamma PN}{1 + \gamma T_h N}$ $\frac{dP}{dt} = -\mu_P P + \frac{F\gamma PN}{1 + \gamma T_h N}$	$2(N,\ P)$	continuous	$X_{\min} = (10, 9.45)$ (fixed point)	$\lambda = 0.2,\ \mu_N = 0.1,\ F = 1$ $\mu_P = 0.1,\ \gamma = 0.01$ $\sigma = 10^{-3},\ T_h = 0.0$
Rosenzweig-MacArthur II	$\frac{dN}{dt} = \left(\lambda - \mu_N + \frac{\sigma}{2}\right)N - \frac{\sigma}{2}N^2 - \frac{\gamma PN}{1 + \gamma T_h N}$ $\frac{dP}{dt} = -\mu_P P + \frac{F\gamma PN}{1 + \gamma T_h N}$	$2(N,\ P)$	continuous	$X_{\min} < 10^{-10}$ (limit cycle)	$\lambda = 0.2,\ \mu_N = 0.1,\ F = 1$ $\mu_P = 0.1,\ \gamma = 0.01$ $\sigma = 10^{-3},\ T_h = 0.0$ $\sigma = 2 \times 10^{-6},\ T_h = 0.5$
Rosenzweig-MacArthur III	$\frac{dN}{dt} = \left(\lambda - \mu_N + \frac{\sigma}{2}\right)N - \frac{\sigma}{2}N^2 - \frac{\gamma PN}{1 + \gamma T_h N}$ $\frac{dP}{dt} = -\mu_P P + \frac{F\gamma PN}{1 + \gamma T_h N}$	$2(N,\ P)$	continuous	$X_{\min} = (5.5, 5.2)$ (limit cycle)	$\lambda = 0.2,\ \mu_N = 0.1,\ F = 1$ $\mu_P = 0.1,\ \gamma = 0.01$ $\sigma = 10^{-3},\ T_h = 0.0$ $\sigma = 10^{-3}, T_h = 0.565$
Rosenzweig-MacArthur IV (Lotka-Volterra)	$\frac{dN}{dt} = (\lambda - \mu_N)N - \gamma PN$ $\frac{dN}{dt} = -\mu_P P + \gamma PN$	$2(N,\ P)$	continuous	$X_{\min} = (0, 0)$ (0, 0) neutral	$\lambda = 0.2,\ \mu_N = 0.1,\ F = 1$ $\mu_P = 0.1,\ \gamma = 0.01$ $\sigma = 10^{-3},\ T_h = 0.0$ $\sigma = 0, T_h = 0$

Notes: In the single-species models, X refers to the population density. In the Nicholson-Bailey model, H and P refer to the host and parasite densities, respectively, while in the Rosenzweig-MacArthur model, N and P refer to the prey and predator densities, respectively. See *Modeling schemes* for clarification of variables.

the number of individuals is the nearest integer to $n_t = e^r x_t$ and the probability of survival is $p_t = e^{-r(x_t/\kappa)}$. When κ is large, random fluctuations in births and deaths are negligible, and since the mean of $B(n_t, p_t)$ is $p_t n_t$, the stochastic Ricker model converges to its deterministic representation. In order to facilitate the numerical methods, we chose parameters such that n_t will always be an integer ($r = \log(17) \approx 2.83$).

After the reaction step described in the previous paragraph, we calculated the diffusion step. Every individual in every patch emigrates with probability given by D, and is randomly allotted among all possible destinations (neighboring patches in the stepping-stone topology and all other patches in the fully connected topology; see Fig. 1). In order to avoid an artificial drift due to updating order, dispersal takes place via a parallel updating scheme (all emigrants leave all patches at the same instant to ensure that the same individual cannot emigrate twice within a time step).

For the continuous-time models we used an event-driven simulation approach based on the Gillespie algorithm (Gillespie 1976), which we extended to incorporate a metapopulation framework. The Gillespie algorithm assigns relative rates to all possible demo-

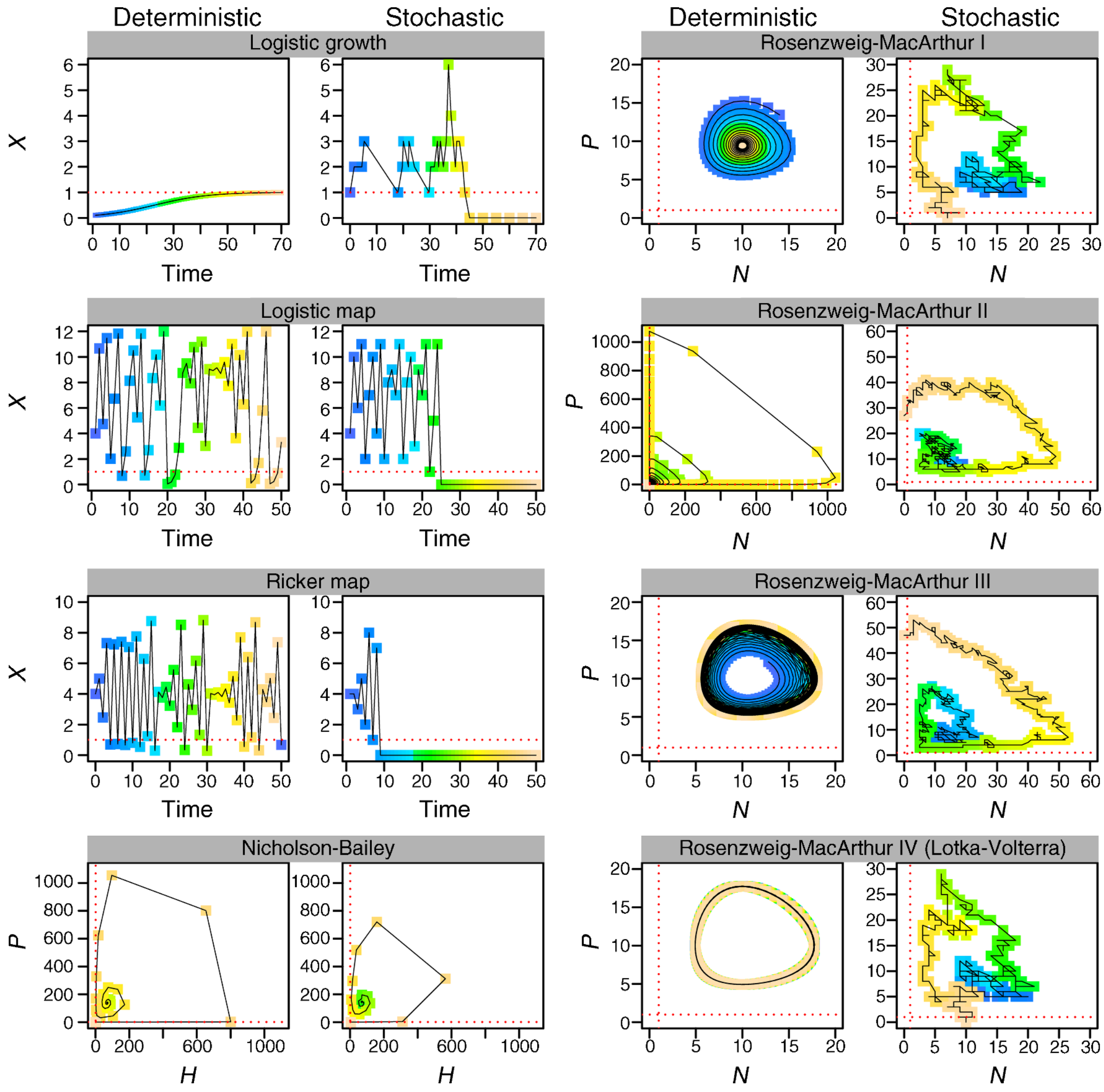

FIG. 2. The "deterministic" behavior of the population dynamics models vs. their single-patch stochastic equivalents. Five population dynamics models were studied with different dynamical features (see Table 1). The time evolution of these models is plotted once for the deterministic case and once for a typical stochastic realization. Time is color coded where blue refers to earlier times and yellow to later ones. The dotted lines are plotted to illustrate the threshold of a single animal, below which the discrete system will reach extinction. In the single-species models, X refers to the population density. In the Nicholson-Bailey model, H and P refer to the host and parasite densities, respectively, while in the Rosenzweig-MacArthur model, N and P refer to the prey and predator densities, respectively.

graphic events (birth, death, predation, dispersal, and so on) that are given by the representative functions, parameters, and current state (population size) of the continuous-time model. For example, for the Logistic growth model,

$$\frac{dx}{dt} = \left(\lambda - \mu + \frac{\sigma}{2}\right)x - \frac{\sigma}{2}x^2 \qquad (2)$$

the (population) birth rate is λx, and the (population) death rate is

$$\mu x + \frac{\sigma}{2}(x^2 - x).$$

Note that alternative representations where the density dependence is in the birth term, or in both terms, can also be used. One event is then selected at random (given their relative probability) and the population state is updated (e.g. a birth corresponds to the addition of a single individual). After the event, the simulation clock is advanced by a random number drawn from an exponential distribution with a parameter equal to the sum of all demographic rates; thus, as the number and rate of events increases (e.g. with larger population size or higher growth rate), the time between demographic events decreases. At large population sizes the event-

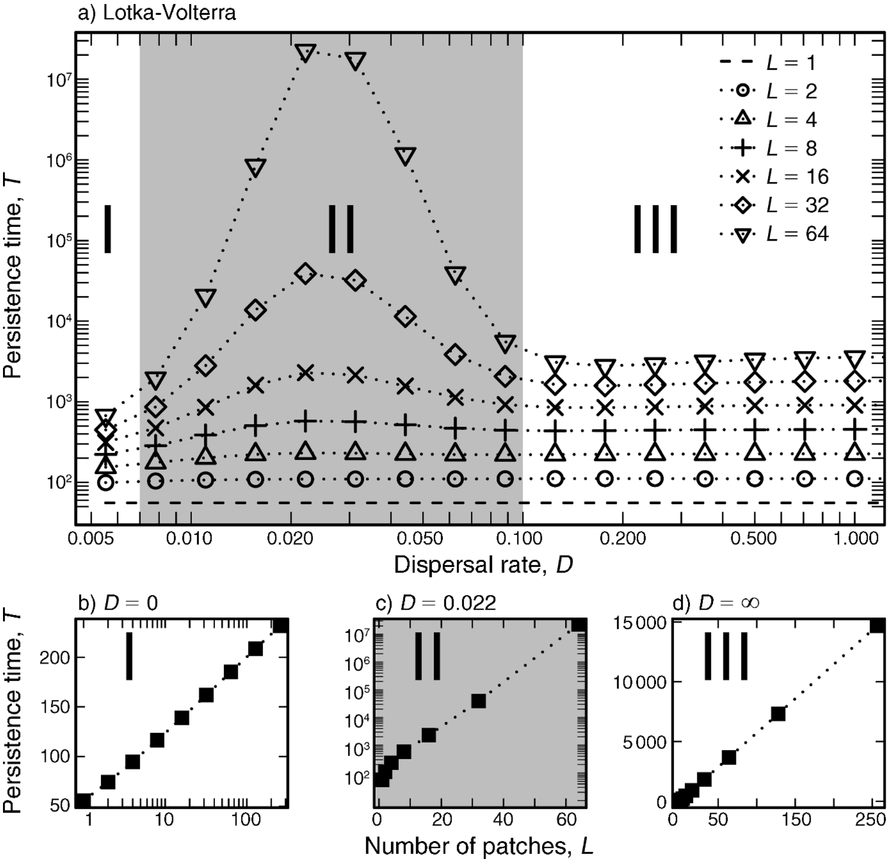

FIG. 3. Scaling of mean metapopulation persistence time (T) vs. patch number (L) for the three dispersal regimes. In the upper panel, T is plotted against the (per capita) dispersal rate (D) for different system sizes (L) for the Lotka-Volterra model embedded in a fully connected topology. The three dispersal regimes (weak, intermediate, and strong) are shaded with different levels of gray and are denoted by I, II, and III, respectively. Both axes have a log scale. The lower panels (b–d) show T vs. L in the three dispersal regimes: (b) in the weak regime, T scales logarithmically with L (which is shown on a logarithmic scale); (c) in the intermediate regime, T (logarithmic scale) scales exponentially with L; and (d) in the strong regime, scaling is nonuniversal. Here, the marginally stable dynamics of the Lotka-Volterra system impose a linear scaling of T with L.

driven simulations converge to the deterministic solution of the ordinary differential equation model on which they are based.

We embedded the dispersal term in the event-driven simulation framework and, as in the discrete-time case, emigrants were randomly assigned to available destinations as defined in the second paragraph of this section. Stochastic analogues of the deterministic models for a single site are shown (a typical realization) in Fig. 2.

Numerical simulations

We factorially combined the six deterministic models, metapopulation sizes (in most cases, 2 to 64 patches by powers of two; in the other cases where T (mean persistence time) was too large to simulate in a reasonable time, we limited the considered sizes to smaller numbers), and the two metapopulation topologies. For each combination we performed between 10^5 and 10^6 simulations. Simulations were initialized at the nearest integer to the nontrivial fixed point (which was unstable for some models) and allowed to run until the population reached zero individuals (in the two-species model we stopped the simulation when one of the populations went extinct). For the Logistic map we initialized the system randomly between 1 and $\kappa - 1$. We calculated the mean persistence time for each combination. For the continuous-time models shown in Fig. 2, we used R package odesolve (Setzer 2008); for discrete models and stochastic simulations, custom programs were written in C/C++ using Gnu Scientific Library (GSL; Galassi et al. 2003) and were analyzed using R (R Development Core Team 2010). All stochastic simulations were carried out using a high-performance cluster (Bulldog K, Yale University, New Haven, Connecticut, USA) consisting of 1536 Intel Xeon (E5410) cores.

RESULTS

All models, with the exception of the continuous-time Logistic growth model, exhibited a maximum in the mean persistence time of the metapopulation at an intermediate dispersal rate (Figs. 3 and 4, and Appendix). As the number of patches in the metapopulation is

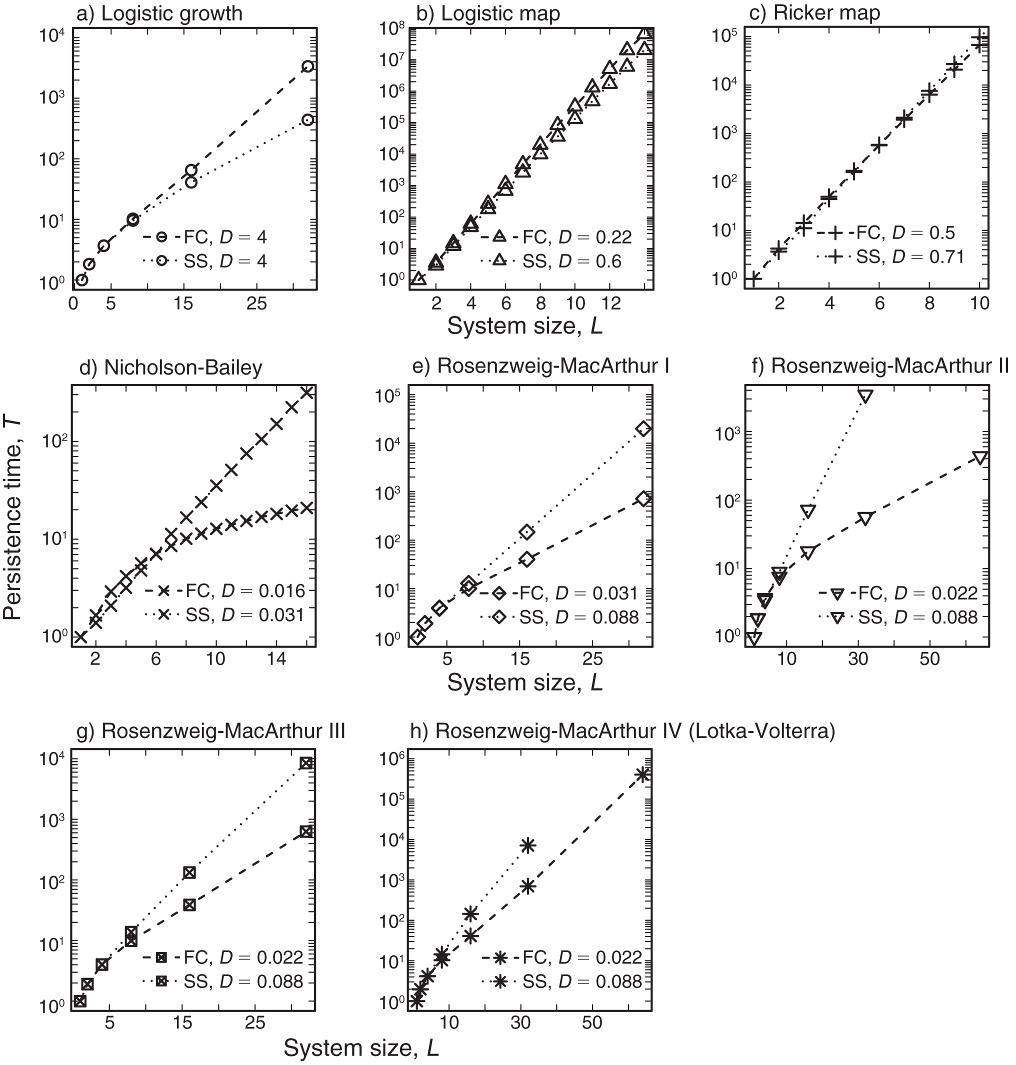

FIG. 4. Scaling relationships for all models in the intermediate-dispersal regime. Under intermediate-dispersal rates, all models demonstrate an exponential scaling of T with L. In all plots, extinction is measured in units of the mean persistence time of a single patch. Dashed lines represent the fully connected (FC) topology, whereas dotted lines represent the stepping-stone (SS) patch topology. In all panels, the y-axis is on a logarithmic scale.

increased, the mean metapopulation persistence time increases for all dispersal rates (Figs. 4–6); however, it increases disproportionately quickly at the dispersal rate that generates the maximum persistence time. In the following sections we describe how the addition of patches interacts with the dispersal rate to generate particular functional (scaling) relationships between metapopulation persistence and number of patches. Because of the generality of this result for all but one model, we discuss the results without reference to specific models (but see the Appendix, where each model is discussed in detail separately).

The effect of patch additions on metapopulation persistence

Adding patches to the metapopulation always increases the mean metapopulation persistence time; however, the form of the relationship between patch number and metapopulation persistence depends on the dispersal rate. In the following sections, we discuss the observed relationship and expectations derived from theory in three dispersal regimes: low, intermediate, and high dispersal, and we describe the characteristic transitions between these regimes.

Low dispersal.—The low-dispersal regime is defined by values of the dispersal rate at which local extinctions occur more quickly, on average, than the rate at which immigrants are received from adjacent patches. This range therefore extends from $D = 0$ to a critical value D_1. Below D_1, the system segregates spontaneously into independent spatial domains, each of these domains may contain one or more patches. These domains are effectively disconnected, and within each domain, the rate of extinction is larger than the rate of colonization.

(Hinrichsen 2000, Keymer et al. 2000, Oborny et al. 2005). The probability that one patch (or one spatial domain) undergoes an extinction at time t is proportional to $\exp(-t/\tau)$, where τ is the mean persistence time (see Appendix). The persistence time of the whole metapopulation is equal to the persistence time of the longest lived of L independent patches or domains. The maximum of L independently and identically distributed random variables from an exponential probability distribution generates a logarithmic relationship between the number of patches L, and the metapopulation persistence time (Ewens and Grant 2005). Fig. 5 shows this logarithmic scaling in the low-dispersal regime for all models studied here. It is important to note that, for most practical purposes, this logarithmic scaling implies that adding more patches will have little noticeable impact on metapopulation persistence.

As D increases from zero towards the critical value D_1, the size and lifetime of the domains increases, but the same considerations still hold. At D_1 a well-understood phase transition occurs (Snyder 2000, Mobilia et al. 2006, Kessler and Shnerb 2010) and the metapopulation forms a single domain, allowing recolonization of an extinct patch even when the nearest occupied patch is many dispersal steps away. This marks the transition to the intermediate-dispersal regime.

Intermediate dispersal.—At intermediate dispersal rates, immigrants arrive in patches more frequently than local extinctions occur, but the dispersal is not strong enough to synchronize local variations across the system. Accordingly, this is the most extinction robust scenario. The lack of synchronization ensures that dynamics (including extinction and recolonization events) occur independently in each patch; moreover, recolonization occurs quickly enough as to ensure a high proportion of patches are typically inhabited. Even when local dynamics are extinction prone, the metapopulation as a whole can exhibit a stable equilibrium (Hastings 1993, Ben-Zion et al. 2010, Kessler and Shnerb 2010), causing the persistence time to scale *exponentially* with the number of patches L. Fig. 4 shows the observed exponential relationship from our simulations in all six models. One way to gain intuition about the form of this relationship is to assume that patches are immediately recolonized after a local extinction. Then, metapopulation extinction requires a regional catastrophe: A stochastic event in which all patches are simultaneously, but in this case independently, driven to extinction. Such an event can be approximated as L independent Bernoulli trials, each with probability p of an extinction. The probability of a global extinction in this case will have probability p^L, which implies that the time until such an extinction will be proportional to p^{-L}, thus giving rise to the observed exponential scaling.

The endpoint of the intermediate-dispersal regime is $D_2(L)$. Above this value, global synchrony occurs and regional catastrophes are no longer rare. If the metacommunity is fully connected this transition occurs sharply (above D_2, independent of the number of patches) as dispersal rate is increased, but for any other topology the number of patches can influence the ability of dispersal to generate global synchrony (Strogatz 1988, Yanchuk 2001); for any fixed dispersal rate, global synchrony collapses above a certain system-size (Earn et al. 2000).

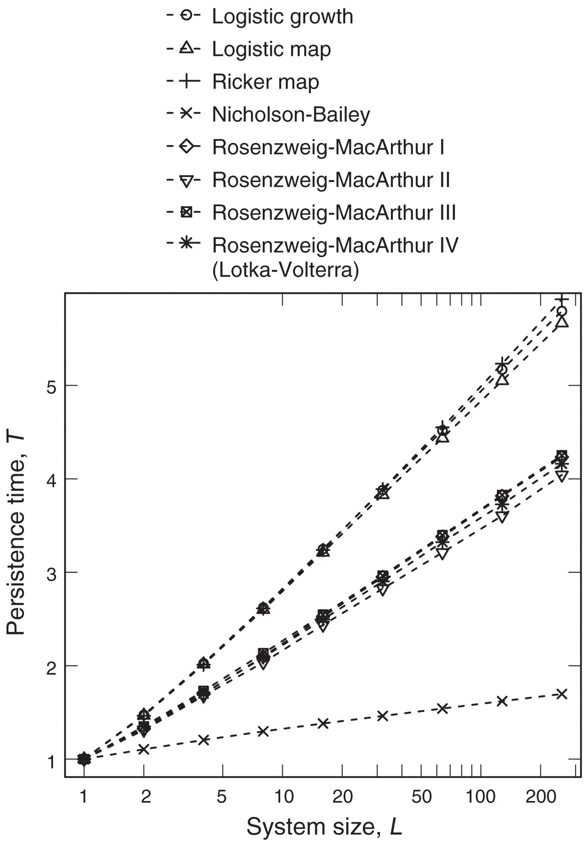

FIG. 5. Scaling relationships for all models in the low-dispersal regime (zero). Under low (zero) dispersal rates, all models demonstrate a logarithmic scaling of persistence time (T) with patch number (L, on a logarithmic scale). In all models, extinction is measured in units of the mean persistence time of a single patch.

High dispersal.—The high-dispersal regime covers the range of dispersal rates that lead to synchronized local dynamics across the entire metapopulation. This regime extends, in the limiting case, to an infinite dispersal rate that is equivalent to assuming that the metapopulation operates as a single large, fully homogenized patch. Increasing the number of patches is equivalent to increasing the carrying capacity of a population inhabiting a single patch (provided that dispersal rates are high enough to ensure that adding patches does not interfere with synchronization). Under these conditions, the scaling of metapopulation persistence time with the number of patches depends upon characteristics of the deterministic dynamics which govern each patch.

An important quantity for determining how increasing patch numbers will alter metapopulation persistence in the high-dispersal regime is the minimum value

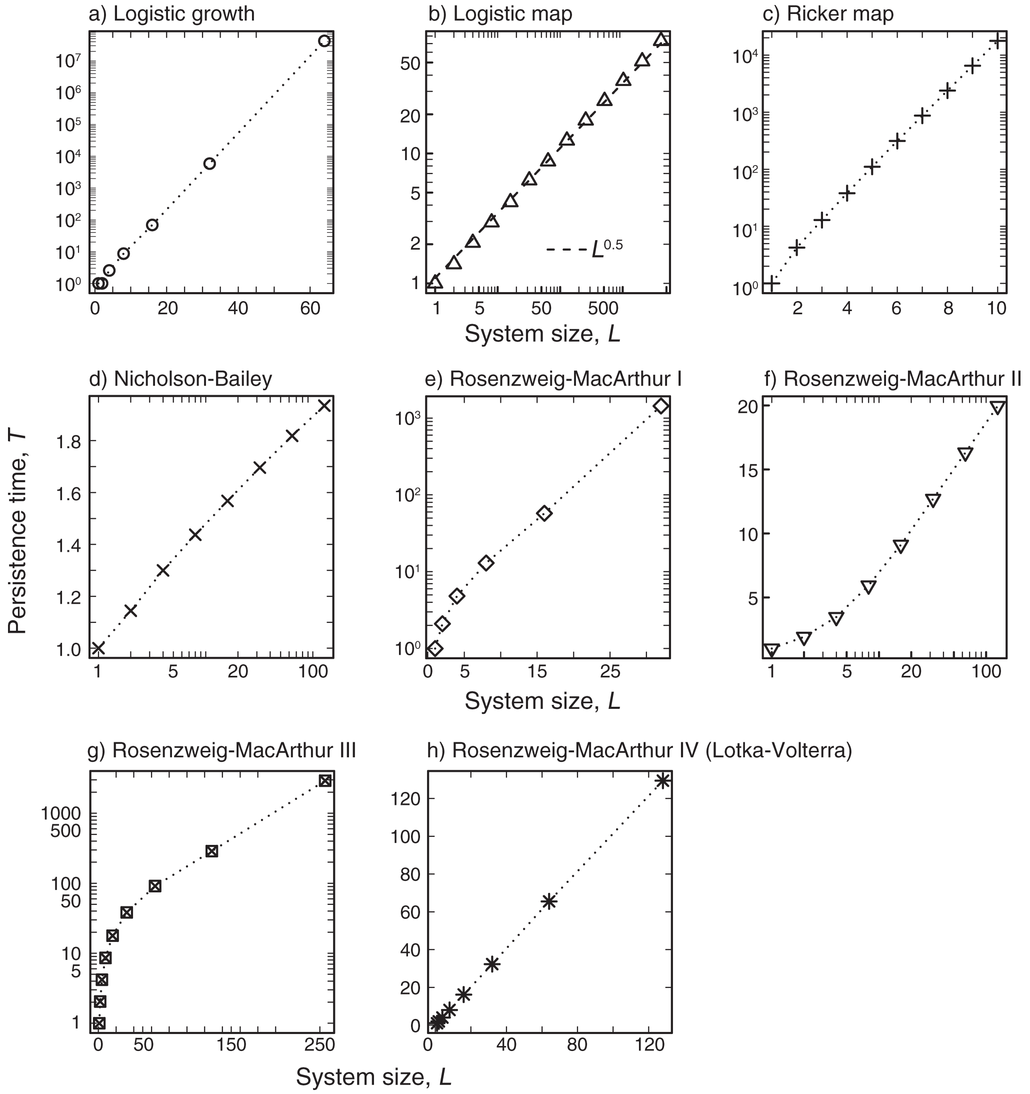

a) Logistic growth

b) Logistic map

c) Ricker map

d) Nicholson-Bailey

e) Rosenzweig-MacArthur I

f) Rosenzweig-MacArthur II

g) Rosenzweig-MacArthur III

h) Rosenzweig-MacArthur IV (Lotka-Volterra)

FIG. 6. Scaling relationships for all models in the high-dispersal regime (infinite). Under high (infinite) dispersal rates, the scaling depends on the properties of the local dynamics (see *Results: High dispersal* and the Appendix for more details and for the rest of the models studied here). In all plots, extinction is measured in units of the mean persistence time of a single patch. T is shown on a logarithmic scale in panels (a)–(c), (e), and (g); L is on a logarithmic scale in panels (b), (d), and (f).

encountered along a trajectory of the deterministic model. We formally define this value, $X_{\min}$, as the minimum value encountered on the deterministic trajectory between $T/2$ and T, as T goes to infinity given that the system was initiated arbitrarily close to zero (for a formal mathematical expression see section 5 in the Appendix). A second important quantity is the variation imposed by demographic stochasticity (or more generally any stochastic component) at or near $X_{\min}$:$\sigma_{X_{\min}}$. The latter component is a compromise between the variation imposed by stochasticity (which for demographic stochasticity is roughly proportional to $\sqrt{X_{\min}}$ and the attractiveness of the deterministic trajectory at that point in time, usually defined as the Lyapunov exponent). Although in some cases it is possible to analytically determine these two quantities, they can both be easily estimated numerically from many realizations of the deterministic and stochastic models. Here we provide a scheme to classify the potential relationships between metapopulation persistence and patch number based on these two quantities (see Fig. 7):

1) $X_{\min} \neq 0$
   a) If $X_{\min} \neq 0$ and $X_{\min} > \sigma_{X_{\min}}$, stochastic trajectories rarely generate extinctions. In this case, the actual probability of extinction can be extracted by measuring the area of a normal distribution with mean and variance $X_{\min}$, which overlaps the extinction boundary (recall that the standard deviation due to demographic stochasticity is approximately $\sqrt{X_{\min}}$ (van Kampen 1992, Lande

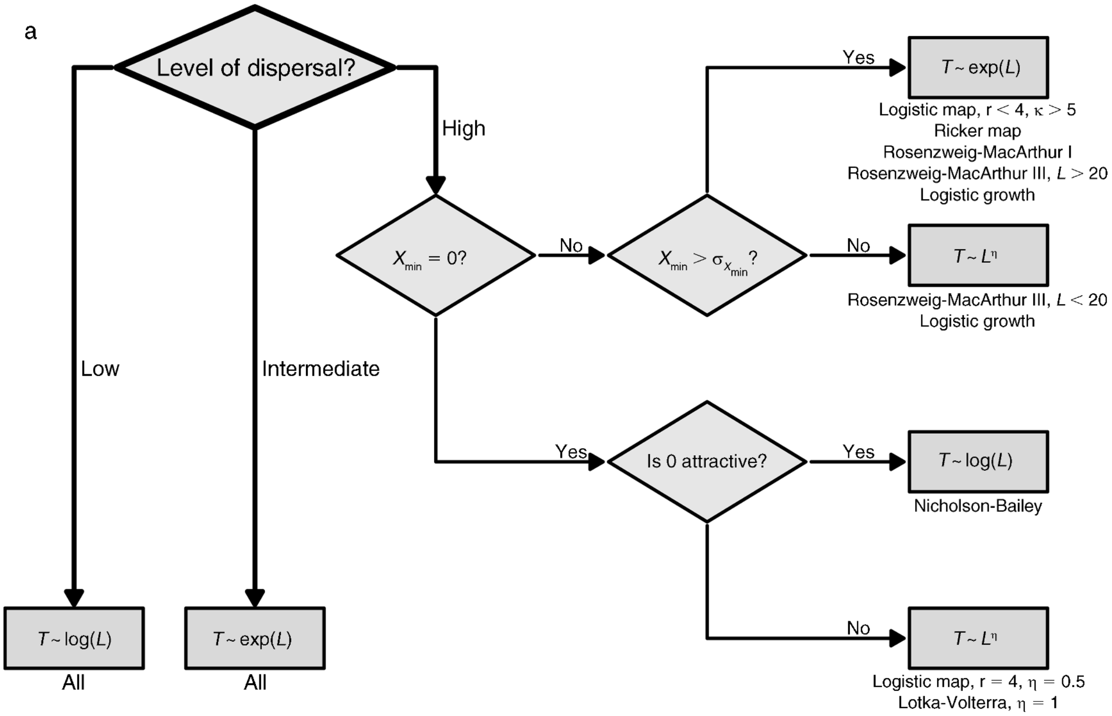

FIG. 7. Flow chart to determine the scaling properties of mean metapopulation persistence time with the number of patches in the high-dispersal regime. The scaling of mean persistence time with patch number depends on the quantities $X_{\min}$ and $\sigma_{X_{\min}}$, which can be estimated deterministically or from time series data (see *Results: High dispersal*). Panel (b) shows an example of a population time series that fits into category 1a in the *Results: High dispersal*; panel (c) shows an example of category 1*b*, panel (d) for category 2a, and panel (e) for category 2b. Abbreviations are: *r*, per capita growth rate; κ, carrying capacity; and η, exponent that govern the power law dependency between mean persistence time (T) and the number of patches (L).

1993). As patches are added to the system, $X_{\min}$ increases and this area decreases exponentially, resulting in an exponential increase of mean persistence time. This logic can be easily extended to multispecies systems by employing a multivariate normal distribution. Examples of this kind in our analysis are Logistic growth, the Ricker map, and Rosenzweig-MacArthur I and III (see Fig. 6).

b) If $X_{\min} \neq 0$ but $X_{\min} \leq \sigma_{X_{\min}}$, stochastic trajectories often lead to extinctions. In this case the initial effect of adding patches to the system will increase metapopulation persistence according to a power law until patch additions yield $X_{\min} > \sigma_{X_{\min}}$, at which point the exponential dependency described in the previous paragraph will occur. Examples of this are Logistic growth and Rosenzweig-MacArthur III until $L = 20$ (Fig. 6 and Appendix).

2) $X_{\min} = 0$

a) Attractive absorbing state: If $X_{\min} = 0$ and zero is also an attractive equilibrium point (as in the Nicholson-Bailey host–parasitoid model), the population size will deterministically flow to less than one individual generating an extinction in the stochastic model. Because the initial rate of population decline increases with initial population size, adding more patches, which is equivalent to a single patch initialized at a larger population size, will result in a logarithmic increase in metapopulation persistence (Fig. 4d).

b) Marginal absorbing state: In most systems, the ratio between $X_{\min}$ to $\sigma_{X_{\min}}$ is a function of the number of patches. However, for some dynamics, $X_{\min}$ is always smaller than $\sigma_{X_{\min}}$. This may happen if $X_{\min} = 0$ (but is not an attractive state), e.g., for the chaotic Logistic map, or when σ may grow unboundedly, like in the marginally stable Lotka-Volterra model. In these cases, the effect of adding more patches increases metapopulation persistence time according to a *power law*. For the Lotka-Volterra model, the power law with exponent equals 1 (Figs. 3 and 6h); this has been previously reported in this system by Reichenbach et al. (2006) and Parker and Kamenev (2009). For the chaotic Logistic map, this relationship depends on the probability of encountering population sizes in the vicinity of the extinction boundary. As the number of patches grows (increasing the effective carrying capacity), the probability of encountering near extinctions decays as approximately as $L^{-1/2}$. Thus, metapopulation persistence grows as a power law with exponent 1/2 (Fig. 6b).

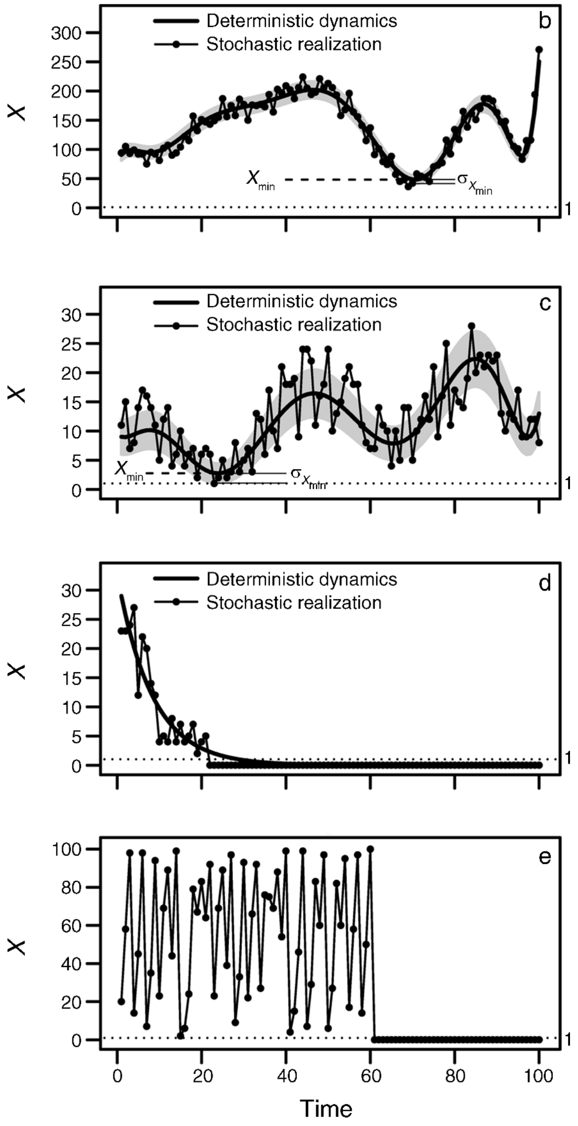

FIG. 7. Continued.

One case worth mentioning is the Rosenzweig-MacArthur II system, in which $X_{\min}$ is extremely small but not zero ($<10^{-10}$). This case behaves effectively like the Nicholson-Bailey system (attractive absorbing state) since we study it with a relatively small number of patches. Ultimately, we expect it to switch to the exponential regime, but the number of patches required to generate this switch is too large to simulate in a finite time.

The effect of topology

In the limiting cases where the dispersal rate is zero or infinite, there is no effect of the connectivity topology on the metapopulation. Likewise, when dispersal is weak or strong (according to our above classifications), topology has a very limited effect. Only when dispersal is intermediate in strength does topology play an important role. Fig. 4 shows that the topology of the system determines the exponent that relates the mean persistence time of the metapopulation to that of a single patch, but does not alter the exponential nature of the relationship between mean persistence time and the number of patches in the metapopulation.

DISCUSSION

Herein we demonstrate that a wide variety of population models have a ubiquitous set of scaling laws determining how metapopulation persistence increases with the number of patches. With weak dispersal (recolonization events are rarer than extinction events) the mean persistence time grows *logarithmically* with the number of patches. However, with intermediate dispersal (recolonization events are more frequent than extinction, but local dynamics remain asynchronous), the mean persistence time grows *exponentially* with the number of patches, even when local dynamics are unstable and extinction prone. When dispersal is strong enough to induce regional coherence in local dynamics, the relationship between mean persistence time and system size depends on the stability of local dynamics; however, it is important to consider that in this regime the metapopulation is acting as a single large homogeneous patch rather than the traditionally defined set of interconnected patches with local demographic processes. In all cases where the stochastic system is made more extinction prone due to synchronization (all models studied here except Logistic growth) intermediate dispersal maximizes persistence. Logistic growth is exceptional since it does not support oscillations, and synchronization does not increase the extinction risk. The other models studied here either support oscillations directly in the form of attractive limit cycles (Rosenzweig-MacArthur II and III) or indirectly as having a focus fixed point (Rosenzweig-MacArthur I, Lotka-Volterra, and Nicholson-Bailey) or their chaotic trajectories oscillate between different domains (Logistic map and Ricker map). Together, these scaling relationships are responsible for the bell-shaped relationship between mean persistence time and dispersal rate observed in metapopulation models (Holyoak and Lawler 1996, Ellner et al. 2001, Kerr et al. 2002, 2006, Kneitel and Miller 2003, Molofsky and Ferdy 2005, Dey and Joshi 2006). A clear prediction arising from our work is that such a relationship should be far more pronounced in systems with a larger number of patches (for an example, see Fig. 3).

The emergence of a common set of scaling laws across single-species and multispecies models, discrete-time and continuous-time models, and stable and unstable local dynamics, suggests the process of demographic extinction in metapopulations is decoupled from local population demography itself. Rather, the scaling of mean persistence time with system size is driven by the colonization–extinction balance that is explicit in many metapopulation models (Levins 1969, Hanski 1991, Barton et al. 1997, Loreau and de Mazancourt 2008), but here arises from mass effects, spatial dynamics, demographic stochasticity, and synchronization. What is surprising is that mass effects have little bearing on the scaling behavior of persistence with system size. Both weak and strong dispersal lead to a paucity of colonization events relative to extinctions; in the former, this is due to low movement rates from extant patches, and in the latter, this is due to a regionally correlated extinction risk leaving few or no recolonists. At some intermediate dispersal rate, the colonization–extinction balance emerges. This alludes to the compelling idea that synchrony (or lack thereof) of populations across a landscape may be a more important feature of the system than population demography itself. Indeed, many authors have already begun to address the importance of synchrony for regional-scale properties of metapopulations and metacommunities (Earn et al. 2000, Earn and Levin 2006, Vasseur and Fox 2009, Gouhier et al. 2010).

Realistic attempts to predict the probability of regional extinction require both demographic and environmentally stochastic elements. Like dispersal, environmental stochasticity has the capacity to generate regional-scale synchrony if it operates at the regional scale (Hanski 1991). In such instances, regional-scale population synchrony could be reached at low to intermediate dispersal rates, leading the metapopulation to behave as a single well-mixed local patch, changing the scaling behavior and sharply reducing mean persistence times. Alternatively, if environmental fluctuations are independent at each local patch, or if population demographics are locally heterogeneous, higher dispersal rates can be tolerated before the system behaves as a single well-mixed system. Moreover, the ability of dispersal to synchronize an entire metapopulation wanes as more patches are added, reducing the likelihood of regional-scale synchrony. Hanski (1991) argued that a logarithmic scaling of persistence time with population size suggested an environmental basis for extinction, whereas exponential scaling suggested a demographic basis for extinction. Our work demonstrates that both patterns can emerge from demographic stochasticity alone when the degree of dispersal is varied from weak to intermediate. When viewed in this light, it is possible that the addition of environmental stochasticity may not generate any novel behaviors in the system, but rescale the action of important parameters like dispersal rate. Nevertheless, a combined approach addressing both demographic and environmental stochasticity may be particularly important when the synchronizing effect of environmental stochasticity does not span the entire region but reaches beyond a single patch.

Current anthropogenic activities are continually fragmenting viable habitats into smaller but potentially more numerous patches. In such cases, calculating the viability of the metapopulation is complicated by a number of confounding impacts including an increased risk of local extinction by demographic stochasticity (Ewers and Didham 2006). Our analysis differs from fragmentation models because the mean risk of local extinction is fixed by the model and parameters, but is independent of the number of patches. Ours is a patch addition rather than patch fragmentation approach, determining the rate at which mean persistence time increases as previously unexploited patches are occupied (or, alternatively, as previously exploited patches are lost from the system). In this respect, one could consider the scaling of mean persistence time as an important proxy for the success of an invader as it undergoes initial range expansion. Extending our approach to cases where patches are fragmented rather than added is a rather obvious and urgently necessary next step. Our demonstration that the scaling properties of metapopulation persistence are conservative across a wide range of local demographic constraints suggests that regional synchronization (or lack thereof) is the most important indicator of sensitivity to patch addition or patch loss. Estimating the local susceptibility to extinction (e.g., Fig. 7) in addition to regional synchronization will provide further insight into metapopulations that are tightly coupled by high dispersal rates.

ACKNOWLEDGMENTS

This work was supported in part by the facilities and staff of the Yale University Faculty of Arts and Sciences High Performance Computing Center. D. A. Vasseur acknowledges the support of Yale University. The work of N. M. Shnerb and Y. Ben-Zion was supported by the Tashtiyot program of the Israeli Ministry of Science and by a BIKURA grant (No. 1026/11) of the Israel Science Foundation (ISF).

LITERATURE CITED

Abbott, K. C. 2011. A dispersal-induced paradox: synchrony and stability in stochastic metapopulations. Ecology Letters 14:1158–1169.

Abta, R., M. Schiffer, A. Ben-Ishay, and N. M. Shnerb. 2008. Stabilization of metapopulation cycles: Toward a classification scheme. Theoretical Population Biology 74:273–282.

Abta, R., M. Schiffer, and N. M. Shnerb. 2007. Amplitude-dependent frequency, desynchro-nization, and stabilization in noisy metapopulation dynamics. Physical Review Letters 98:098104.

Allen, J. C., W. M. Schaffer, and D. Rosko. 1993. Chaos reduces species extinction by amplifying local population noise. Nature 364:229–232.

Barton, N., M. Whitlock, I. Hanski, and M. Gilpin. 1997. The evolutuion of metapopulations. Pages 183–210 *in* I. Hanski and M. Gilpin, editors. Metapopulation biology: ecology, genetics, and evolution. Academic Press, San Diego, California, USA.

Ben-Zion, Y., G. Yaari, and N. M. Shnerb. 2010. Optimizing metapopulation sustainability through a checkerboard strategy. PLoS Computational Biology 6:e1000643.

Bonsall, M. B., and A. Hastings. 2004. Demographic and environmental stochasticity in predator-prey metapopulation dynamics. Journal of Animal Ecology 73:1043–1055.

Brown, J. H., and A. Kodric-Brown. 1977. Turnover rates in insular biogeography: effect of immigration on extinction. Ecology 58:445–449.

Brunet, E., and B. Derrida. 1997. Shift in the velocity of a front due to a cutoff. Physical Review E 56:2597.

Bulte, E. H., and G. C. van Kooten. 1999. Metapopulation dynamics and stochastic bioeconomic modeling. Ecological Economics 30:293–299.

Burkey, T. V. 1997. Metapopulation extinction in fragmented landscapes: using bacteria and protozoa communities as model ecosystems. American Naturalist 150:568–591.

Chesson, P. 2000. General theory of competitive coexistence in spatially-varying environments. Theoretical Population Biology 58:211–237.

Dey, S., and A. Joshi. 2006. Stability via asynchrony in drosophila metapopulations with low migration rates. Science 312:434–436.

Drake, J. M., and B. D. Griffen. 2010. Early warning signals of extinction in deteriorating environments. Nature 467:456–459.

Durrett, R., and S. A. Levin. 1994. The importance of being discrete (and spatial). Theoretical Population Biology 46:363–394.

Earn, D. J. D., and S. A. Levin. 2006. Global asymptotic coherence in discrete dynamical systems. Proceedings of the National Academy of Sciences USA 103:3968–3971.

Earn, D. J. D., S. A. Levin, and P. Rohani. 2000. Coherence and conservation. Science 290:1360–1364.

Elgart, V., and A. Kamenev. 2004. Rare event statistics in reaction-diffusion systems. Physical Review E 70:041106.

Ellner, S. P., E. McCauley, B. E. Kendall, C. J. Briggs, P. R. Hosseini, S. N. Wood, A. Janssen, M. W. Sabelis, P. Turchin, R. M. Nisbet, and W. W. Murdoch. 2001. Habitat structure and population persistence in an experimental community. Nature 412:538–543.

Etienne, R. S., C. J. ter Braak, C. C. Vos, I. Hanski, and O. E. Gaggiotti. 2004. Application of stochastic patch occupancy models to real metapopulations. Pages 105–132 *in* Ecology, genetics and evolution of metapopulations. Academic Press, Burlington, Vermont, USA.

Ewens, W. J., and G. R. Grant. 2005. Statistical methods in bioinformatics: an introduction. Springer, New York, New York, USA.

Ewers, R. M., and R. K. Didham. 2006. Confounding factors in the detection of species responses to habitat fragmentation. Biological Reviews 81:117–142.

Galassi, M., J. Davies, J. Theiler, B. Gough, G. Jungman, M. Booth, and F. Rossi. 2003. Gnu scientific library: reference manual. Network Theory, Bristol, UK.

Gillespie, D. T. 1976. A general method for numerically simulating the stochastic time evolution of coupled chemical reactions. Journal of Computational Physics 22:403–434.

Gouhier, T. C., F. Guichard, and A. Gonzalez. 2010. Synchrony and stability of food webs in metacommunities. American Naturalist 175:E16–E34.

Hanski, I. 1991. Single-species metapopulation dynamics: concepts, models and observations. Biological Journal of the Linnean Society 42:17–38.

Hanski, I., and M. Gilpin. 1991. Metapopulation dynamics: brief history and conceptual domain. Biological Journal of the Linnean Society 42:3–16.

Hanski, I., and O. Ovaskainen. 2000. The metapopulation capacity of a fragmented landscape. Nature 404:755–758.

Hastings, A. 1993. Complex interactions between dispersal and dynamics: lessons from coupled logistic equations. Ecology 74:1362–1372.

Hastings, A., and D. B. Wysham. 2010. Regime shifts in ecological systems can occur with no warning. Ecology Letters 13:464–472.

Heino, M., V. Kaitala, E. Ranta, and J. Lindstrm. 1997. Synchronous dynamics and rates of extinction in spatially structured populations. Proceedings of the Royal Society B 264:481–486.

Hinrichsen, H. 2000. Non-equilibrium critical phenomena and phase transitions into absorbing states. Advances in Physics 49:815–958.

Holyoak, M. 2000. Habitat patch arrangement and metapopulation persistence of predators and prey. American Naturalist 156:378–389.

Holyoak, M., and S. P. Lawler. 1996. Persistence of an extinction-prone predator–prey interaction through metapopulation dynamics. Ecology 77:1867–1879.

Holyoak, M., M. A. Leibold, and R. D. Holt. 2005. Metacommunities: spatial dynamics and ecological communities. University of Chicago Press, Chicago, Illinois, USA.

Johst, K., R. Brandl, and S. Eber. 2002. Metapopulation persistence in dynamic landscapes: the role of dispersal distance. Oikos 98:263–270.

Kamenev, A., and B. Meerson. 2008. Extinction of an infectious disease: A large fluctuation in a nonequilibrium system. Physical Review E 77:061107.

Keeling, M. J. 2002. Using individual-based simulations to test the Levins metapopulation paradigm. Journal of Animal Ecology 71:270–279.

Keeling, M. J., and C. A. Gilligan. 2000. Metapopulation dynamics of bubonic plague. Nature 407:903–906.

Keeling, M. J., H. B. Wilson, and S. W. Pacala. 2000. Reinterpreting space, time lags, and functional responses in ecological models. Science 290:1758–1761.

Kerr, B., C. Neuhauser, B. J. M. Bohannan, and A. M. Dean. 2006. Local migration promotes competitive restraint in a hostpathogen 'tragedy of the commons.' Nature 442:75–78.

Kerr, B., M. A. Riley, M. W. Feldman, and B. J. M. Bohannan. 2002. Local dispersal promotes biodiversity in a real-life game of rock-paper-scissors. Nature 418:171–174.

Kessler, D. A., and H. Levine. 1998. Fluctuation-induced diffusive instabilities. Nature 394:556–558.

Kessler, D. A., and N. M. Shnerb. 2007. Extinction rates for fluctuation-induced meta-stabilities: a real-space WKB approach. Journal of Statistical Physics 127:861–886.

Kessler, D. A., and N. M. Shnerb. 2008. Novel exponents control the quasi-deterministic limit of the extinction transition. Journal of Physics A: Mathematical and Theoretical 41:292003.

Kessler, D. A., and N. M. Shnerb. 2010. Globally coupled chaotic maps and demographic stochasticity. Physical Review E-Statistical, Nonlinear, and Soft Matter Physics 81:036111.

Keymer, J. E., P. A. Marquet, J. X. VelascoHernndez, and S. A. Levin. 2000. Extinction thresholds and metapopulation persistence in dynamic landscapes. American Naturalist 156:478–494.

Kneitel, J. M., and T. E. Miller. 2003. Dispersal rates affect species composition in meta-communities of *Sarracenia purpurea* inquilines. American Naturalist 162:165–171.

Lande, R. 1993. Risks of population extinction from demographic and environmental stochasticity and random catastrophes. American Naturalist 142:911–927.

Legendre, S., T. W. Schoener, J. Clobert, and D. A. Spiller. 2008. How is extinction risk related to population size variability over time? A family of models for species with repeated extinction and immigration. American Naturalist 172:282–298.

Levins, R. 1969. Some demographic and genetic consequences of environmental heterogeneity for biological control. Bulletin of the ESA 15(4):237–240.

Levins, R. 1970. Some mathematical questions in biology. Pages 75–107 *in* M. Gerstenhaber, editor. Lectures on mathematics in life sciences. American Mathematical Society, Providence, Rhode Island, USA.

Loreau, M., and C. de Mazancourt. 2008. Species synchrony and its drivers: neutral and nonneutral community dynamics in fluctuating environments. American Naturalist 172:E48–E66.

Loreau, M., N. Mouquet, and A. Gonzalez. 2003. Biodiversity as spatial insurance in heterogeneous landscapes. Proceedings of the National Academy of Sciences USA 100:12765–12770.

Martin, K., P. B. Stacey, and C. E. Braun. 2000. Recruitment, dispersal, and demographic rescue in spatially-structured white-tailed ptarmigan populations. Condor 102:503–516.

Matthies, D., I. Bruer, W. Maibom, and T. Tscharntke. 2004. Population size and the risk of local extinction: empirical evidence from rare plants. Oikos 105:481–488.

May, R. M. 1973. Stability in randomly fluctuating versus deterministic environments. American Naturalist 107:621–650.

Missel, A. R., and K. A. Dahmen. 2008. Hopping conduction and bacteria: transport in disordered reaction-diffusion systems. Physical Review Letters 100:058301.

Mobilia, M., I. T. Georgiev, and U. C. Tuber. 2006. Fluctuations and correlations in lattice models for predator-prey interaction. Physical Review E 73:040903.

Molofsky, J., and J. Ferdy. 2005. Extinction dynamics in experimental metapopulations. Proceedings of the National Academy of Sciences USA 102:3726–3731.

Oborny, B., G. Meszna, and G. Szab. 2005. Dynamics of populations on the verge of extinction. Oikos 109:291–296.

Ovaskainen, O., and B. Meerson. 2010. Stochastic models of population extinction. Trends in Ecology and Evolution 25:643–652.

Parker, M., and A. Kamenev. 2009. Extinction in the Lotka-Volterra model. Physical Review Letters 80:021129.

R Development Core Team. 2010. R: a language and environment for statistical computing. R Foundation for Statistical Computing, Vienna, Austria. http://www.R-project.org

Reichenbach, T., M. Mobilia, and E. Frey. 2006. Coexistence versus extinction in the stochastic cyclic Lotka-Volterra model. Physical Review E 74:051907.

Setzer, R. W. 2008. odesolve: solvers for ordinary differential equations. R Foundation for Statistical Computing, Vienna, Austria. http://cran.r-project.org/web/packages/odesolve/

Shmida, A., and M. V. Wilson. 1985. Biological determinants of species diversity. Journal of Biogeography 12:1–20.

Snyder, R. 2000. Spatial structure and fluctuations in the contact process and related models. Bulletin of Mathematical Biology 62:959–975.

Sokolov, I. M., J. Mai, and A. Blumen. 1997. Paradoxal diffusion in chemical space for nearest-neighbor walks over polymer chains. Physical Review Letters 79:857–860.

Stacey, P. B., and M. Taper. 1992. Environmental variation and the persistence of small populations. Ecological Applications 2:18–29.

Strogatz, S. 1988. Phase-locking and critical phenomena in lattices of coupled nonlinear oscillators with random intrinsic frequencies. Physica D: Nonlinear Phenomena 31:143–168.

van Kampen, N. G. 1992. Stochastic processes in physics and chemistry. Elsevier, Amsterdam, The Netherlands.

Vasseur, D. A., and J. W. Fox. 2009. Phase-locking and environmental fluctuations generate synchrony in a predator–prey community. Nature 460:1007–1010.

Yanchuk, S. 2001. Partial synchronization and clustering in a system of diffusively coupled chaotic oscillators. Mathematics and Computers in Simulation 54:491–508.

zu Dohna, H., and M. Pineda-Krch. 2010. Fitting parameters of stochastic birth–death models to metapopulation data. Theoretical Population Biology 78:71–76.

Supplemental Material

Appendix

Details of numerical procedures and further analysis of the specific models considered (*Ecological Archives* E093-104-A1).